

Two-site dynamical mean-field theory

Michael Potthoff*

Institut für Physik, Humboldt-Universität zu Berlin, 10115 Berlin, Germany

(Received 19 February 2001; published 8 October 2001)

It is shown that a minimum realization of the dynamical mean-field theory (DMFT) can be achieved by mapping a correlated lattice model onto an impurity model in which the impurity is coupled to an uncorrelated bath that consists of a single site only. The two-site impurity model can be solved exactly. The mapping is approximate. The self-consistency conditions are constructed in a way that the resulting “two-site DMFT” reduces to the previously discussed linearized DMFT for the Mott transition. It is demonstrated that a reasonable description of the mean-field physics is possible with a minimum computational effort. This qualifies the simple two-site DMFT for a systematic study of more complex lattice models which cannot be treated by the full DMFT in a feasible way. To show the strengths and limitations of the new approach, the single-band Hubbard model is investigated in detail. The predictions of the two-site DMFT are compared with results of the full DMFT. Internal consistency checks are performed which concern the Luttinger sum rule, other Fermi-liquid relations and thermodynamic consistency.

DOI: 10.1103/PhysRevB.64.165114

PACS number(s): 71.10.Fd, 71.10.Hf, 71.30.+h

I. INTRODUCTION

The dynamical mean-field theory (DMFT) has become a well-established and valuable method to investigate the physics of strongly correlated electrons on a lattice.^{1–4} Similar to the Weiss mean-field theory for classical models of localized spins, the DMFT is exact in the nontrivial limit of infinite spatial dimensions.^{5,6} For finite dimensions it provides a thermodynamically consistent and nonperturbative mean-field approach in which the spatial correlations are neglected but the temporal degrees of freedom are treated correctly. The application of the DMFT to the single-band Hubbard model^{7–9} has uncovered a complex phenomenology which may be characterized by strongly renormalized Fermi-liquid behavior competing with the Mott insulating state and with different kinds of spontaneous order such as collective magnetism.^{3,4,10–12}

The DMFT actually consists in a prescription that maps the original lattice model onto an effective impurity model which describes a single correlated impurity orbital embedded in an uncorrelated bath of conduction-band states. This mapping is a self-consistent one, namely, the bath parameters depend on the on-site lattice Green function. The impurity model is the crucial point in the DMFT since it poses a highly nontrivial many-body problem that must be solved repeatedly. The different methods employed for an essentially exact solution of the impurity model, the quantum Monte Carlo,^{2,13} the exact diagonalization,^{14,15} and the numerical renormalization-group methods^{16,17} work well for the single-band Hubbard model but are computationally expensive. In practice this severely limits the applicability of the DMFT, particularly when one is concerned with multiband models. More complex lattice models including two, three or more degenerate or nondegenerate d -like bands possibly hybridized with uncorrelated s - p -like bands are interesting for obvious reasons. For example, multiband models are required for a minimum theory of the physics of strongly correlated electrons in the transition-metal oxides. Because of the large parameter space and the complexity of the effec-

tive impurity problem, a detailed and systematic calculation of the phase diagrams of multiband models covering the entire parameter space is far beyond the ability of present implementations of the DMFT.

If one is interested in a comprehensive mean-field description of complex lattice models but wishes to keep the essence of the DMFT, some compromise is inevitable. In principle, there are only two possibilities conceivable. First, one may refrain from a numerically exact solution of the impurity problem and employ approximate treatments instead. These may be based on different limits where a small parameter is available. This idea has been pursued with weak- and strong-coupling perturbational approaches such as the iterative perturbation theory^{1,18,19} or the noncrossing approximation.^{20,21,12} In fact, multiband Hubbard-type models can be treated in this way with an acceptable computing time (see Refs. 22,23, for examples). This route, however, shall not be followed up here.

The present paper takes into consideration the only alternative left, namely to solve the impurity model exactly but to reduce the number of bath degrees of freedom to keep the calculations manageable. There are no problems to treat, e.g., the single-impurity Anderson model (SIAM) with a small number of sites n_s numerically exact. On the other hand, for any finite $n_s < \infty$ the self-consistent mapping of the Hubbard model onto the SIAM is approximate. The exact solution of the effective impurity model is thus achieved at the expense of an approximate self-consistency.

As a function of n_s the Hilbert-space dimension D of the impurity model increases exponentially. It is given by $D = 2^{2M}$ where M is the number of (twofold spin-degenerate) one-particle orbitals. The self-consistent mapping within the DMFT at least requires $M = r + r(n_s - 1) = rn_s$ orbitals for the case of one impurity site, $n_s - 1$ bath sites, and r correlated bands (see the Appendix). Consider, for example, the d -band of a $3d$ transition metal with a twofold degenerate e_g -derived band and a threefold degenerate t_{2g} -derived band. In this case $M = 5n_s$ orbitals have to be considered. Accepting $M = 10$ as a typical value for the maximum number of

orbitals that can be taken into account for a repeated solution of the impurity model within a reasonable computing time, limits n_s to the smallest number that is reasonable: $n_s=2$, i.e., an impurity model with one impurity site and one bath site.

The purpose of the present paper is to test whether or not a two-site DMFT could be a meaningful approach and to show up its strengths and limitations. There are mainly two tasks to be performed: First, it is necessary to specify the approximate self-consistent mapping. This means to find a sensible prescription how to fix the bath parameters of the impurity model—guided by the original self-consistency condition of the DMFT. Second, the resulting two-site DMFT has to be tested against the full DMFT. This can be done best for the single-band Hubbard model (in infinite dimensions) where numerous essentially exact results are available. Thus, except for a short discussion of the extension of the theory to multiband systems, the present paper is exclusively concerned with the single-band model. Since one cannot expect a strongly simplified two-site approach to reproduce the known results quantitatively exact, the present study attaches importance to main trends, qualitative correctness and internal consistency. Recall that even the full DMFT cannot be expected to give more than a qualitative (mean-field) description of the physics of transition-metal oxides.

The two-site SIAM has been considered within the context of the DMFT beforehand. Lange²⁴ discussed the two-site SIAM at half-filling to investigate renormalized versus unrenormalized perturbational approaches to the DMFT of the Mott transition. However, a self-consistent mapping of the Hubbard model onto the two-site SIAM was not considered. Bulla and Potthoff²⁵ developed a linearized DMFT of the Mott transition. The Hubbard model at half-filling and at the critical interaction strength $U=U_c$ was self-consistently mapped onto the two-site SIAM resulting in a linear algebraic mean-field equation. The solution of the two-site SIAM is exact, the mapping is approximate. It was found that, compared with the full DMFT, the linearized DMFT gives fairly good analytical estimates for U_c on different lattices. The theory, however, is restricted to the critical point. Further extensions of the linearized DMFT for the Mott transition have been developed for a periodic Anderson model by Held and Bulla²⁶ and for a two-band Hubbard model by Ono *et al.*²⁷ Extensions of the linearized DMFT to the Hubbard model for thin films²⁸ and semi-infinite lattices²⁹ have convincingly shown that the main trends in the geometry dependence of U_c can be predicted safely. Here, it will be shown that a two-site DMFT can be constructed which is not bound to the (Mott) critical point but is able to access the entire parameter space and that reduces to the linearized DMFT at half-filling and $U=U_c$.

The paper is organized as follows. The next section gives a brief review of the DMFT and introduces the self-consistent two-site approach. Section III presents a variety of results for the single-band Hubbard model starting with the Mott transition. Hereafter, the Fermi-liquid phase off half filling is addressed, and the Luttinger sum rule, other Fermi-liquid relations and thermodynamical consistency are dis-

cussed. A discussion of the two-site DMFT in relation to other methods and the conclusions are given in Sec. IV. The generalization of the theory to multiband models is presented in the Appendix.

II. TWO-SITE DYNAMICAL MEAN-FIELD THEORY

To be definite the single-band Hubbard model on the Bethe lattice with infinite connectivity $q \mapsto \infty$ is considered:

$$H = \sum_{\langle ij \rangle \sigma} t_{ij} c_{i\sigma}^\dagger c_{j\sigma} + \frac{U}{2} \sum_{i\sigma} n_{i\sigma} n_{i-\sigma}. \quad (1)$$

The hopping is assumed to be non-zero between nearest neighbors i and j only. $t \equiv -t_{ij} > 0$ is the nearest-neighbor hopping integral. The on-site hopping $t_0 \equiv t_{ii}$ is set to $t_0 = 0$ to fix the energy zero. Furthermore, U is the on-site Coulomb interaction, $c_{i\sigma}^\dagger$ creates an electron at the site i with spin $\sigma = \uparrow, \downarrow$, and $n_{i\sigma} = c_{i\sigma}^\dagger c_{i\sigma}$. With the usual scaling of the hopping, $t = t^*/\sqrt{q}$ and $t^* = \text{const}$, the model is nontrivial in the limit $q \mapsto \infty$.⁵ Setting $t^* = 1$ fixes the energy scale for the present paper. For a paramagnetic, spatially homogeneous phase the on-site Green function $G(\omega) = \langle\langle c_{i\sigma}; c_{i\sigma}^\dagger \rangle\rangle_\omega$ is given by

$$G(\omega) = \int_{-\infty}^{\infty} dx \frac{\rho_0(x)}{\omega + \mu - x - \Sigma(\omega)}, \quad (2)$$

where μ is the chemical potential, and $\Sigma(\omega)$ is the self-energy which is local (\mathbf{k} independent) in the limit $q \mapsto \infty$.^{5,30} $\rho_0(x)$ denotes the free density of states

$$\rho_0(x) = \frac{1}{2\pi t^{*2}} \sqrt{4t^{*2} - x^2} \quad (3)$$

for $|x| < 2t^*$. The bandwidth is $W = 4t^* = 4$.

A. Dynamical mean-field theory

The DMFT essentially rests on the observation that the local self-energy is given by a (skeleton-diagram) functional $\Sigma = \mathcal{S}[G]$ of the on-site Green function that is universal for a large class of models. Consider, in particular, the single-impurity Anderson model (SIAM):

$$H_{\text{imp}} = \sum_{\sigma} \epsilon_d d_{\sigma}^{\dagger} d_{\sigma} + U d_{\uparrow}^{\dagger} d_{\uparrow} d_{\downarrow}^{\dagger} d_{\downarrow} + \sum_{\sigma, k=2}^{n_s} \epsilon_k a_{k\sigma}^{\dagger} a_{k\sigma} + \sum_{\sigma, k=2}^{n_s} V_k (d_{\sigma}^{\dagger} a_{k\sigma} + \text{H.c.}), \quad (4)$$

which describes an impurity orbital $d_{\sigma}^{\dagger}|0\rangle$ with one-particle energy ϵ_d and on-site interaction U that is coupled via the hybridization V_k to a bath of $n_s - 1$ noninteracting orbitals $a_{k\sigma}^{\dagger}|0\rangle$ with energies ϵ_k . The impurity Green function $G_{\text{imp}}(\omega) = \langle\langle d_{\sigma}; d_{\sigma}^{\dagger} \rangle\rangle_{\omega}$ is given by

$$G_{\text{imp}}(\omega) = \frac{1}{\omega + \mu - \epsilon_d - \Delta(\omega) - \Sigma_{\text{imp}}(\omega)}, \quad (5)$$

where $\Delta(\omega) = \sum_{k=2}^{n_s} V_k^2 / (\omega + \mu - \epsilon_k)$ is the hybridization function, and $\Sigma_{\text{imp}}(\omega)$ the impurity self-energy. As usual, $\epsilon_d = t_0 = 0$. The important point is that the functional \mathcal{S} is the same as for the Hubbard model, $\Sigma_{\text{imp}} = \mathcal{S}[G_{\text{imp}}]$, because the same type of skeleton diagrams occur in the expansion of Σ_{imp} . Choosing the bath parameters ϵ_k and V_k such that

$$\Delta(\omega) = \omega + \mu - \epsilon_d - \Sigma_{\text{imp}}(\omega) - \frac{1}{G(\omega)}, \quad (6)$$

i.e., such that the DMFT self-consistency condition

$$G_{\text{imp}}(\omega) = G(\omega), \quad (7)$$

is fulfilled, then at once

$$\Sigma_{\text{imp}}(\omega) = \Sigma(\omega). \quad (8)$$

Therewith, the original lattice problem is mapped onto the SIAM and can be solved by the following iterative procedure: Starting with a guess for the local self-energy, the on-site lattice Green function is calculated from Eq. (2). Via Eq. (6) or Eq. (7) the Green function and the self-energy define the hybridization function $\Delta(\omega)$ and thus the parameters of the effective SIAM. Finally, the impurity problem is solved to get a new estimate for the self-energy. The cycles have to be repeated until self-consistency is achieved.

B. Two-site SIAM

The self-consistency condition (7) can be fulfilled rigorously only for $n_s \rightarrow \infty$, i.e., for a bath with an infinite number of degrees of freedom. This leads to the usual SIAM which represents an involved many-body problem. To simplify the problem and to construct a two-site DMFT, the case $n_s = 2$ is considered here, i.e., an effective SIAM that consists of one impurity site and one bath site only. This represents the most simple bath conceivable.

For $n_s = 2$ the site index is fixed to the value $k = 2$ in Eq. (4). There are only two independent bath parameters left, the one-particle energy of the bath site $\epsilon_c \equiv \epsilon_{k=2}$ and the hybridization strength $V \equiv V_{k=2}$. The hybridization function is a one-pole function

$$\Delta(\omega) = V^2 / (\omega + \mu - \epsilon_c), \quad (9)$$

and the free ($U = 0$) impurity Green function is a two-pole function

$$G_{\text{imp}}^{(0)}(\omega) = \frac{1}{2r} \left(\frac{r + \bar{\epsilon}}{\omega + \mu - \bar{\epsilon} - r} + \frac{r - \bar{\epsilon}}{\omega + \mu - \bar{\epsilon} + r} \right), \quad (10)$$

with $\bar{\epsilon} \equiv (\epsilon_d - \epsilon_c)/2$ and $r = \sqrt{\bar{\epsilon}^2 + V^2}$. The interacting impurity Green function $G_{\text{imp}}(\omega)$ has four poles and the self-energy $\Sigma_{\text{imp}}(\omega)$ two poles in general. Closed analytical expressions can be derived for the symmetric model at half-filling (see Ref. 24, for example). For the nonsymmetric case the model can be solved straightforwardly by numerical means without any problems.

For clarity, the theory will be developed for the paramagnetic phase of single-band Hubbard model. However, it is

rather straightforward to consider in essentially the same way also different magnetic phases and/or more complicated models such as multiband Hubbard-type models, for example.

C. Self-consistency

For the two-site DMFT the Eqs. (2)–(5) and Eq. (8) are retained. The original self-consistency condition (7), however, must be reformulated. This means to find two physically motivated (self-consistency) conditions to fix the bath parameters ϵ_c and V .

Consider first the limit of high frequencies $\omega \rightarrow \infty$. The exact self-energy of the impurity problem (4) can be expanded in powers of $1/\omega$:

$$\Sigma(\omega) = Un_d + \frac{U^2 n_d (1 - n_d)}{\omega} + \mathcal{O}(1/\omega^2), \quad (11)$$

where $n_d = n_{d\sigma}$ is the average occupancy of the impurity orbital

$$n_d = \langle d_{\sigma}^{\dagger} d_{\sigma} \rangle = -\frac{1}{\pi} \int_{-\infty}^0 \text{Im} G_{\text{imp}}(\omega + i0^+) d\omega. \quad (12)$$

Inserting the expansion (11) into Eq. (2), one finds the following high-frequency expansion of the on-site lattice Green function:

$$G(\omega) = \frac{1}{\omega} + \frac{t_0 - \mu + Un_d}{\omega^2} + \frac{M_2^{(0)} + (t_0 - \mu)^2 + 2(t_0 - \mu)Un_d + U^2 n_d}{\omega^3} + \mathcal{O}(1/\omega^4). \quad (13)$$

Here $M_2^{(0)} = \sum_{j \neq i} t_{ij}^2 = \int dx x^2 \rho_0(x)$ is the variance of the noninteracting density of states (3). Equation (13) can be compared with the exact high-frequency expansion which is available by calculating the first nontrivial moments of the interacting density of states.³¹ One finds that Eq. (13) in fact represents the exact expansion provided that $n_{\text{imp}} \equiv 2n_d$ can be identified with the filling $n = \langle n_{i\uparrow} \rangle + \langle n_{i\downarrow} \rangle$ of the lattice model. It is therefore required that

$$n_{\text{imp}} = n, \quad (14)$$

where the band filling is calculated via

$$n = -\frac{2}{\pi} \int_{-\infty}^0 \text{Im} G(\omega + i0^+) d\omega. \quad (15)$$

Equation (14) is the first self-consistency condition. The high-frequency behavior of $G(\omega)$ is important for the occurrence and for the correct weights and centers of gravity of the two high-frequency Hubbard excitations in the spectrum. With Eqs. (12), (14), and (15), an integral form of the original self-consistency equation (7) is fulfilled: $\int_{-\infty}^0 d\omega \text{Im} G = \int_{-\infty}^0 d\omega \text{Im} G_{\text{imp}}$.

Consider now the low-frequency limit $\omega \rightarrow 0$. The exact self-energy of the impurity problem (4) can be expanded in powers of ω ,

$$\Sigma(\omega) = a + b\omega + \mathcal{O}(\omega^2), \quad (16)$$

with constants a and b . The definition $z = 1/(1-b)$ will be convenient, i.e.,

$$z = \frac{1}{1 - d\Sigma(0)/d\omega}. \quad (17)$$

For a metal z has the meaning of the quasi-particle weight. Neglecting terms of the order ω^2 , and inserting into Eq. (2) yields $G(\omega) = G^{(\text{coh})}(\omega)$ for small ω where $G^{(\text{coh})}(\omega)$ is the coherent part of the on-site Green function defined as

$$\begin{aligned} G^{(\text{coh})}(\omega) &= \int_{-\infty}^{\infty} dx \frac{\rho_0(x)}{\omega + \mu - x - a - b\omega} \\ &= z \int_{-\infty}^{\infty} dx \frac{\rho_0(x)}{\omega - z(x - \mu + a)}. \end{aligned} \quad (18)$$

On the other hand, the coherent part of the impurity Green function is

$$\begin{aligned} G_{\text{imp}}^{(\text{coh})}(\omega) &= \frac{1}{\omega + \mu - \epsilon_d - \Delta(\omega) - a - b\omega} \\ &= z \frac{1}{\omega - z[\epsilon_d - \mu + a + \Delta(\omega)]}. \end{aligned} \quad (19)$$

Comparing the *high*-frequency expansions of the respective coherent Green functions

$$\begin{aligned} G^{(\text{coh})}(\omega) &= \frac{z}{\omega} + \frac{z^2(t_0 - \mu + a)}{\omega^2} \\ &\quad + \frac{z^3[M_2^{(0)} + (t_0 - \mu + a)^2]}{\omega^3} + \mathcal{O}(1/\omega^4) \end{aligned} \quad (20)$$

and

$$\begin{aligned} G_{\text{imp}}^{(\text{coh})}(\omega) &= \frac{z}{\omega} + \frac{z^2(\epsilon_d - \mu + a)}{\omega^2} + \frac{z^2V^2 + z^3(\epsilon_d - \mu + a)^2}{\omega^3} \\ &\quad + \mathcal{O}(1/\omega^4), \end{aligned} \quad (21)$$

leads to the second self-consistency condition

$$V^2 = zM_2^{(0)}. \quad (22)$$

Thereby, the original self-consistency equation (7) is also fulfilled at low frequencies up to $\mathcal{O}(\omega)$ in an *integral* way, namely by referring to the weight, the center of gravity and the variance of the coherent quasi-particle peak. Equations (14) and (22) reformulate the high- and the low-frequency range of the original self-consistency condition (7) in an integral, qualitative form and are thus well motivated.

D. Calculations

With the two conditions (14) and (22) the two bath parameters are fixed and can be calculated self-consistently: Consider the model parameters t_0 , t , U , μ , and $\rho_0(x)$ to be given. Starting with a guess for ϵ_c and V , the two-site impurity model (4) is well defined and can be solved to find the average occupancy of the impurity level n_{imp} and the self-energy $\Sigma(\omega)$. The latter directly yields the quasiparticle weight $z = [1 - d\Sigma(0)/d\omega]^{-1}$ and from the condition (22) a new value for the hybridization strength V . Inserting $\Sigma(\omega)$ into Eq. (2), gives the on-site lattice Green function $G(\omega)$ and, via Eq. (15), the filling n which has to be compared with n_{imp} . Finally, a new value for ϵ_c is chosen such that the difference $n - n_{\text{imp}}$ is reduced in the next cycle—according to condition (14). The cycles have to be iterated until ϵ_c and V are self-consistent (and $n_{\text{imp}} = n$).

In most cases, one finds a self-consistent set of bath parameters ϵ_c and V such that the ground state of the effective SIAM lies in the six-dimensional subspace characterized by the total spin-dependent particle numbers $N_{\uparrow} = N_{\downarrow} = 1$. To get the self-energy, it is convenient to calculate $G_{\text{imp}}(\omega)$ from its Lehmann representation and to use the Dyson equation in reverse:

$$\Sigma(\omega) = G_{\text{imp}}^{(0)}(\omega)^{-1} - G_{\text{imp}}(\omega)^{-1}, \quad (23)$$

where the free impurity Green function is taken from Eq. (10). The calculation of the eigenenergies and eigenstates is straightforward, but even for $n_s = 2$ this can only be done numerically in general. From the computational point of view, the most time-consuming step, however, is the calculation of the filling from Eqs. (2) and (15). Since the self-energy of the two-site impurity problem is a real two-pole function of the form

$$\Sigma(\omega) = \alpha_0 + \frac{\alpha_1}{\omega - \omega_1} + \frac{\alpha_2}{\omega - \omega_2}, \quad (24)$$

the filling can be calculated more directly by a single one-dimensional integration

$$n = 2 \int_{-\infty}^0 d\omega \rho_0[\omega + \mu - \Sigma(\omega)]. \quad (25)$$

$\rho(\omega) \equiv \rho_0[\omega + \mu - \Sigma(\omega)]$ is the interacting density of states. Since even a repeated evaluation of this equation during the search for self-consistency is not very crucial, extremely fast numerical calculations can be performed.

The two-site DMFT is obviously exact in the limits $n = 0$ and $n = 2$. In the empty-band limit, for example, the impurity self-energy vanishes since $n_{\text{imp}} = n = 0$. Furthermore, it is exact in the band limit $U = 0$. In the atomic limit $t = 0$ one finds $V = 0$ (and arbitrary ϵ_c) to be a self-consistent solution. Since $n = n_{\text{imp}}$, the self-energy is given by

$$\Sigma_{H=1}(\omega) = U \frac{n}{2} + \frac{U^2(n/2)(1-n/2)}{\omega + \mu - t_0 - U(1-n/2)}, \quad (26)$$

which is the correct atomic-limit self-energy. Hence, the two-site DMFT is also exact for $t = 0$ and any filling. Since Eq.

(26) is the Hubbard-I self-energy,⁷ the theory reduces to the Hubbard-I approach whenever there is a self-consistent solution with $V=0$. Actually, this is realized only at half-filling $n=1$ and for sufficiently strong U (see below).

Although the original lattice problem is mapped onto an effective impurity problem with a finite number of degrees of freedom, the dependence of physical quantities, such as the filling n , on the model parameters will generally be smooth. Consider, for example, the function $n(\mu)$ for a given U . The interacting impurity spectral function generally consists of four isolated δ peaks of different weight. An infinitesimal change of μ is unlikely to cause a finite jump of n_{imp} since a change of n_{imp} is in first place caused by a redistribution of spectral weight among the δ peaks rather than by μ crossing a pole. Bearing in mind that the bath parameters itself depend on μ , the function $n(\mu)$ can be continuous even in a large μ interval. In fact, it is found that the chemical potential never crosses a pole except for some extreme cases ($n=0, n=2, V=0$).

III. RESULTS

The two-site DMFT provides a very simple, computationally fast and nonperturbative mean-field approach to correlated lattice models. To show its strengths and limitations, numerical results will be presented for the single-band Hubbard model which has been studied extensively by the full DMFT in the past.^{1-6,10-23} This will set the basis for a discussion of the approach and a comparison with other methods in Sec. IV. Multiband models are considered in the Appendix. The calculations have been performed for the Bethe lattice with infinite connectivity q . The free density of states is given by Eq. (3). Its width is $W=4$.

A. Mott transition

For the symmetric case of half filling $n=1$ and $\mu=U/2$, the approach can be evaluated analytically. Particle-hole symmetry requires $\epsilon_c=U/2=\mu$ to ensure the first self-consistency equation $n=n_{\text{imp}}$. Thus, only the hybridization strength V has to be calculated self-consistently.

Let us first consider the critical point for the Mott transition, i.e., $U \mapsto U_c$ where the linearized DMFT is recovered (see Ref. 25): Coming from the weak-coupling, metallic side, the critical interaction U_c is characterized by a vanishing quasiparticle weight $z \mapsto 0$ which, according to Eq. (22) implies $V \mapsto 0$. In this limit two of the four poles of the impurity Green function are located near $\omega = \pm U/2$ while two poles lie close to $\omega=0$. Referring to the latter, the quasiparticle weight z can be calculated as the sum of their weights. A straightforward calculation to leading order in V yields

$$z = 2 \frac{18V^2}{U^2}. \quad (27)$$

On the other hand, another relation between z and V is given by the second self-consistency condition (22). This implies

$$V^2 = M_2^{(0)} \frac{36}{U^2} V^2, \quad (28)$$

namely, a simple *linear* homogeneous mean-field equation as is characteristic for the linearized DMFT of Ref. 25. A non-trivial solution of this equation is only possible for $U=U_c$ where

$$U_c = 6 \sqrt{M_2^{(0)}}. \quad (29)$$

The second moment of $\rho_0(x)$ is easily calculated: $M_2^{(0)} = \sum_{j \neq i} t_{ij}^2 = qt^2 = t^{*2} = 1$, and therewith $U_c = 6t^* = 1.5W$. This result of the linearized DMFT is very close to the result of the projective self-consistent method (PSCM),^{4,32} $U_c = 1.46W$, and to the result of the numerical renormalization-group (NRG) calculation,¹⁷ $U_c = 1.47W$. The linearized DMFT is able to predict very reliably the main trends in the dependence of U_c on the lattice geometry even for systems with reduced translational symmetry.^{25,28,29,26}

The two-site DMFT is not restricted to the critical point $U=U_c$ but more general. For $\mu=U/2$ and $n=1$ the self-energy of the two-site SIAM can be calculated analytically:²⁴

$$\Sigma(\omega) = \frac{U}{2} + \frac{U^2}{8} \left(\frac{1}{\omega - 3V} + \frac{1}{\omega + 3V} \right). \quad (30)$$

With Eq. (17) this gives the quasiparticle weight

$$z = \frac{1}{1 + U^2/36V^2}, \quad (31)$$

consistent with Eq. (27) for $V \mapsto 0$. Together with the self-consistency condition (22) one arrives at

$$V^2 = \frac{M_2^{(0)}}{1 + U^2/36V^2}. \quad (32)$$

This algebraic but nonlinear mean-field equation has the self-consistent solution

$$V = \sqrt{M_2^{(0)} - \frac{U^2}{36}} \quad (33)$$

for $U < 6 \sqrt{M_2^{(0)}} = U_c$ and $V=0$ else. This yields the U dependence of the quasiparticle weight at half filling:

$$z = 1 - \frac{U^2}{U_c^2}. \quad (34)$$

The result is the same as in the Gutzwiller variational approach³³

$$z_{\text{BR}} = 1 - \frac{U^2}{U_{c,\text{BR}}^2}. \quad (35)$$

However, the Brinkman-Rice critical interaction $U_{c,\text{BR}} = -16 \int_{-\infty}^0 dx x \rho_0(x) \approx 6.79t^* > 6t^*$ is considerably stronger.

The result of the two-site DMFT is compared with the Brinkman-Rice solution and with the results of numerical

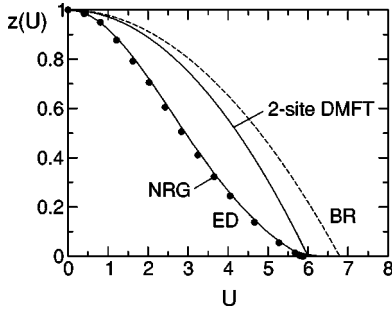


FIG. 1. U dependence of the quasiparticle weight at half-filling as obtained within the two-site DMFT, the Brinkman-Rice approach (Ref. 33) (dashed), the exact-diagonalization method (Refs. 14,34) (solid), and the numerical renormalization-group approach (Ref. 17) (dots).

solutions of the full DMFT by using the exact-diagonalization method^{14,34} ($n_s = 8$ sites) and the NRG (Ref. 17) in Fig. 1. There is a good agreement between the results of the ED and the NRG calculations except for interactions close to U_c where the energy scale of the quasiparticle resonance cannot be resolved reliably within the ED method. The two-site DMFT overestimates the quasi-particle weight in the whole U range. However, the qualitative agreement with the full DMFT is better than could be expected for the rather simple approach and clearly improves on the result of the Gutzwiller method.

The two-site DMFT interpolates between the trivial $U = 0$ limit and $U = U_c$. For $U = U_c$ it is a reasonable approximation to neglect (i) the influence of the Hubbard bands at high frequencies on the low-frequency (quasiparticle) peak and (ii) the internal structure of the quasiparticle peak (see the discussion in Ref. 25). These are just the basic assumptions of the linearized DMFT which the two-site approach reduces to for $U = U_c$. For $0 < U < U_c$ these assumptions are less justified. Yet, the quadratic behavior of $z(U)$ for $U \rightarrow 0$ as well as the eventually linear behavior for $U \rightarrow U_c$ is consistent with the findings of the ED and NRG calculations.

For $U > U_c$ the self-consistent solution is given by $V = 0$ which implies that the two-site DMFT reduces to the Hubbard-I approach in this case [Eq. (26)]. This is a crude description of the Mott insulator, even if compared with the Hubbard alloy-analogy solution and the iterative perturbation theory. The main deficiency is that the widths of the Hubbard bands are largely underestimated (see Ref. 35, for example).

B. Fillings

$n \neq 1$ For the symmetric case $n = 1$ the first self-consistency equation $n = n_{\text{imp}}$ is fulfilled trivially by particle-hole symmetry since $\epsilon_c = U/2 = \mu$, and only the hybridization strength V has to be determined self-consistently. For a thorough test of the two-site DMFT it is thus necessary to consider fillings off half filling, too.

Figure 2 shows the self-consistent bath parameters ϵ_c and V as a function of the filling for $U = 4$. As U is smaller than U_c the hybridization strength is finite for $n = 1$. For decreasing filling the system becomes less and less correlated, and

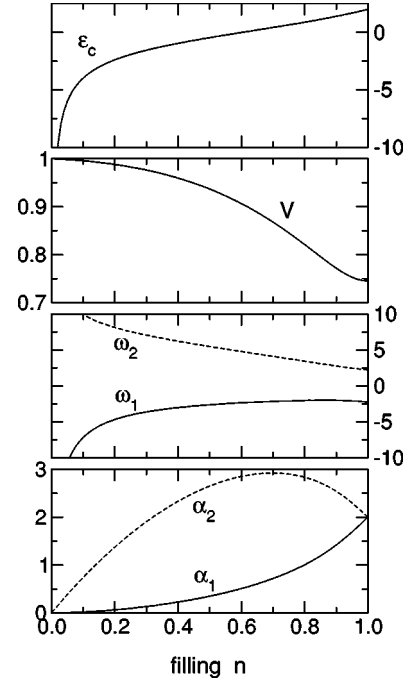


FIG. 2. Filling dependence of the parameters of the effective two-site impurity model ϵ_c and V and of the poles ω_1 , ω_2 and respective weights α_1 , α_2 of the self-energy [see Eq. (24)]. $U = W = 4$.

consequently V has to increase until $V = 1 = M_2^{(0)}$ for $n = 0$. According to Eq. (22) this implies the correct value $z = 1$ for the quasiparticle weight in the empty-band limit. At half-filling the one-particle energy of the bath site is given by $\epsilon_c = 2 = U/2$. It decreases with decreasing filling n and diverges on approaching the empty-band limit $\epsilon_c \rightarrow -\infty$, as is necessary to ensure a vanishing occupancy of the impurity orbital $n_{\text{imp}} = n \rightarrow 0$ for finite V . Note that both parameters ϵ_c and V are smooth functions of the filling.

Off half-filling the interacting impurity Green function continues to have four poles for $U > 0$ and two poles for $U = 0$. This implies that the self-energy is a two-pole function of the form (24) not only for half-filling but also for $n \neq 1$. The poles ω_1 and ω_2 of the self-energy and their respective weights α_1 and α_2 are shown in the lower panels of Fig. 2. Again, it is noteworthy that these are smooth functions connecting the symmetric point $n = 1$ where $\omega_1 + \omega_2 = 0$ and $\alpha_1 = \alpha_2$ with the empty-band limit where the poles become irrelevant since $\alpha_1, \alpha_2 \rightarrow 0$.

It is well known⁴ that the density of states in the paramagnetic phase of the infinite-dimensional Hubbard model essentially consists of three peaks, the lower and the upper Hubbard band and a quasiparticle resonance in the vicinity of the Fermi energy. An attractive feature of the two-site DMFT is that this general form of the density of states can be reproduced qualitatively. It is obvious that the two-pole structure of the self-energy results in a three-peak structure of the density of states (DOS) $\rho(\omega) \equiv \rho_0[\omega + \mu - \Sigma(\omega)]$.

Because the two-pole self-energy is real, the Hubbard bands and the quasiparticle resonance will be perfectly separated from each other on the real frequency axis. Clearly, this

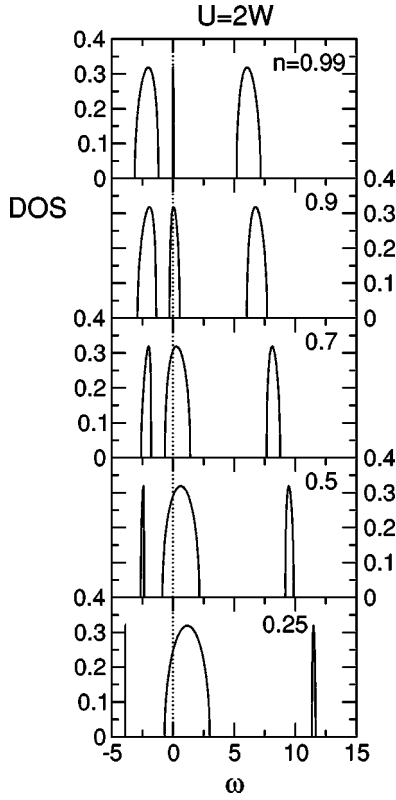


FIG. 3. Density of states $\rho(\omega)$ for $U=2W=8$ and different fillings.

is only a sketch of the true density of states—the full DMFT generally predicts the resonance to merge with one of the Hubbard peaks.^{36,4,18,19} The symmetric case at half-filling is an exception. For $U < U_c$ but close to U_c , a more or less clear separation of energy scales is found to be realized in fact.^{4,17}

Results for the DOS are shown in Fig. 3 for $U=2W=8$ at different fillings. Since $U > U_c$ in this case, the Mott insulator is approached for $n \rightarrow 1$. As soon as there is a finite hole concentration $1-n$, a quasi-particle resonance appears the width of which becomes broader with decreasing filling. The resonance is pinned to the Fermi energy. For the symmetric case $n=1$ and $U < U_c$ it has a maximum at $\omega=0$. For decreasing $n < 1$ the maximum shifts to a frequency $\omega_0 > 0$, and the asymmetry with respect to $\omega=0$ increases. Concurrently, the upper Hubbard band shifts to higher frequencies while its weight decreases. All this is qualitatively correct when comparing with the full DMFT.^{36,4,18} However, the two-site DMFT largely underestimates the widths of the Hubbard bands and does not predict the quasiparticle resonance to merge with the lower Hubbard band not even for smaller fillings. This is an obvious artifact.

The width of the resonance is determined by z . The filling dependence of the quasiparticle weight is shown in Fig. 4 for different U . For $n \rightarrow 0$ there is a linear trend of the quasiparticle weight $z-1 \propto n$. For $n \rightarrow 1$ the weight $z(n)$ behaves linearly when $U > U_c$ and quadratically when $U < U_c$. Generally, z is a monotonously decreasing function of the filling for $n < 1$ and arbitrary U and a monotonously decreasing

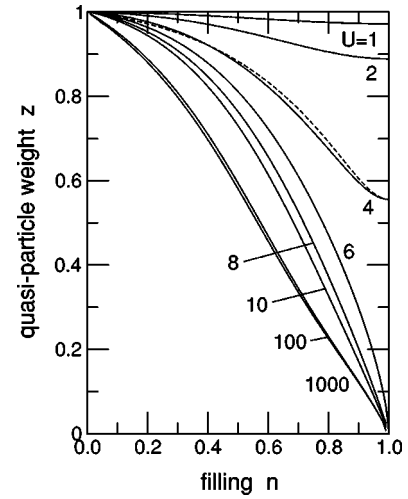


FIG. 4. Quasiparticle weight as a function of the filling for different interaction strengths. Dashed line: calculation for $U=4$ with a slightly modified theory (see text).

function of U for arbitrary n which saturates in the limit $U \rightarrow \infty$. These results are very similar to those of the Gutzwiller approach^{8,37,38} and qualitatively reproduce the results of the full DMFT (Ref. 34) while quantitatively there are deviations similar as for the case $n=1$ which has been discussed already (see Fig. 1).

The same holds for the filling dependence of the internal energy E , the double occupancy $d \equiv \langle n_\uparrow n_\downarrow \rangle$ and the chemical potential μ which is shown in Fig. 5. For $U=W=4$ as well

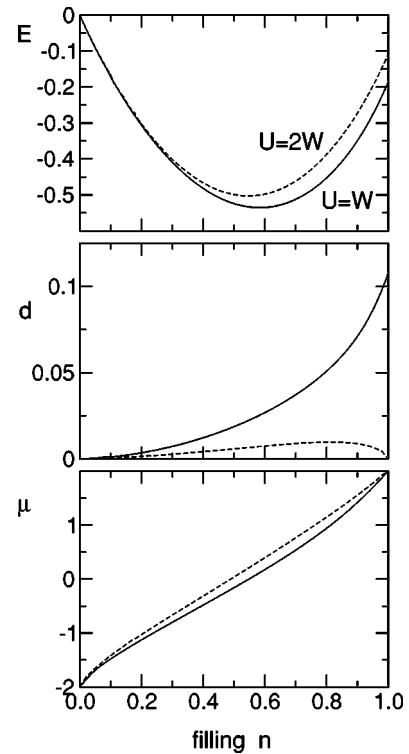


FIG. 5. Filling dependence of the total energy E , the double occupancy $d = \langle n_\uparrow n_\downarrow \rangle$, and the chemical potential μ . Results for $U=W$ (solid lines) and $U=2W$ (dashed lines).

as for $U=2W=8$ the chemical potential monotonously increases with increasing filling as it is required by thermodynamic stability. From the equation of motion for the on-site lattice Green function one can derive simple expressions for the kinetic energy per site

$$E_{\text{kin}} = 2 \int_{-\infty}^0 d\omega [\omega + \mu - \Sigma(\omega)] \rho(\omega), \quad (36)$$

and for the potential energy per site

$$E_{\text{pot}} = \int_{-\infty}^0 d\omega \Sigma(\omega) \rho(\omega). \quad (37)$$

The internal energy per site is given by $E = E_{\text{kin}} + E_{\text{pot}}$, and the average number of doubly occupied sites by $d \equiv \langle n_{\uparrow} n_{\downarrow} \rangle = E_{\text{pot}}/U$. The double occupancy vanishes in the strong-coupling limit $U \rightarrow \infty$. For $U = W < U_c$ it is a monotonously increasing function of n while d is small (but nonzero) for $U = 2W > U_c$ at half filling.

C. Test of Fermi-liquid relations

Opposed to the full DMFT, the two-site DMFT is not a conserving approach in the sense of Baym and Kadanoff.³⁹ Consequently, the two-site DMFT cannot be expected to respect certain exact Fermi-liquid relations.⁴⁰ Drastic violations of the Luttinger theorem and Fermi-liquid relations for the charge and spin susceptibilities are well known⁴¹ for simple nonconserving theories such as the Hubbard-I approximation,⁷ the Roth two-pole approximation,⁴² or the spectral-density approach,⁴³ for example. For the two-site DMFT it is shown here that there are violations of Fermi-liquid relations indeed. Surprisingly, however, these are fairly small.

One important property of a Fermi liquid is that the self-energy $\Sigma(\omega)$ is real at $\omega=0$, i.e., $\text{Im} \Sigma(i0^+) = 0$. This guarantees the existence of a Fermi surface which (for a Bravais lattice) is defined by the set of points in \mathbf{k} space with $0 = \mu - \epsilon(\mathbf{k}) - \Sigma(0)$ where $\epsilon(\mathbf{k})$ is the free band dispersion. The Luttinger sum rule⁴⁰ states that the volume enclosed by the Fermi surface

$$V_{\text{FS}} = 2 \sum_{\mathbf{k}} \Theta[\mu - \epsilon(\mathbf{k}) - \Sigma(0)], \quad (38)$$

is equal to the average particle number:

$$V_{\text{FS}} = \langle N \rangle. \quad (39)$$

Here, Θ is the usual step function, and $\langle N \rangle = \langle \sum_{i\sigma} n_{i\sigma} \rangle = Ln$ where L is the number of lattice sites. The Fermi-surface volume can be calculated in the following way:

$$\begin{aligned} V_{\text{FS}}/L &= 2 \int_{-\infty}^{\infty} dx \rho_0(x) \Theta[\mu - x - \Sigma(0)] \\ &= 2 \int_{-\infty}^0 dx \rho_0[x + \mu - \Sigma(0)] \end{aligned} \quad (40)$$

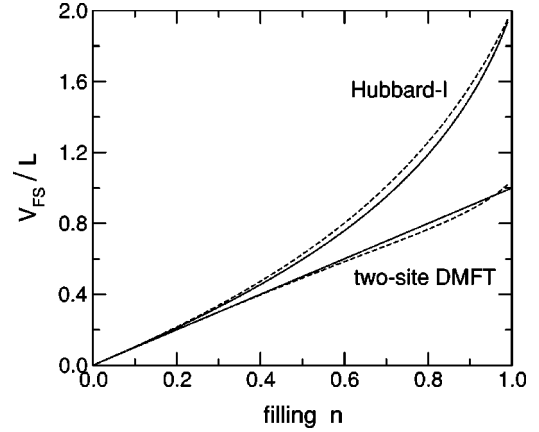


FIG. 6. Normalized “Fermi-surface volume” V_{FS}/L as a function of the filling n for $U=W$ (solid lines) and $U=2W$ (dashed lines). Results as obtained within the two-site DMFT and the Hubbard-I approximation.

to be compared with the filling as given by Eq. (25). The equation $V_{\text{FS}}/L = n$ with V_{FS}/L given by Eq. (40) is a reformulation of the Luttinger sum rule that is also valid for the Bethe lattice.

In Fig. 6 the Fermi-surface volume V_{FS}/L is compared with the filling n for different U . For moderate interactions ($U=W$, solid line) the Luttinger theorem $V_{\text{FS}}/L = n$ is almost exactly fulfilled in the whole range of fillings while deviations of a few percent are found for strong Coulomb interaction ($U=2W$, dashed line) near half filling. The results of the Hubbard-I approach are shown for comparison. It is seen that in this case the Fermi-surface volume is strongly overestimated up to a factor 2 near half filling and irrespective of U .

An alternative formulation of the Luttinger theorem is given by³⁰

$$\mu = \mu_0 + \Sigma(0), \quad (41)$$

where μ_0 is the chemical potential for $U=0$. Replacing the first self-consistency equation (14) by Eq. (41), defines a variant of the two-site DMFT where the Luttinger theorem is enforced. The resulting filling dependence of the quasiparticle weight is shown in Fig. 4 for $U=4$ by the dashed line. If the original two-site DMFT respected the Luttinger theorem, there would not be any difference compared with the result of the variant. As is seen in Fig. 4, the difference is nonzero but rather small.

By means of perturbation theory to all orders⁴⁰ the compressibility or charge susceptibility

$$\kappa = \frac{\partial n}{\partial \mu} \quad (42)$$

can be shown to be related to the DOS and the self-energy at $\omega=0$:

$$\kappa = 2\rho(0) \left(1 - \frac{\partial \Sigma(0)}{\partial \mu} \right). \quad (43)$$

Similarly, the spin susceptibility

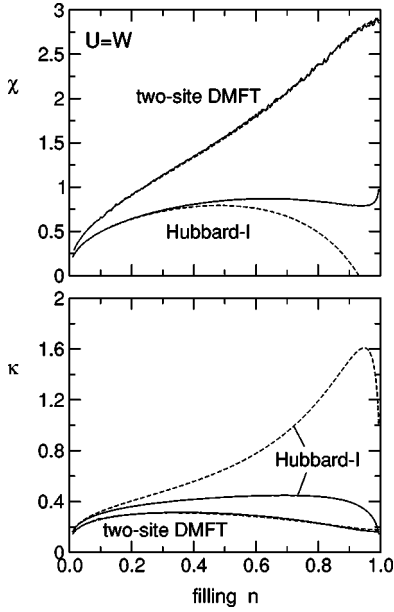


FIG. 7. Charge susceptibility (compressibility) κ and spin susceptibility χ as functions of the filling for $U=W=4$. Results for the two-site DMFT and the Hubbard-I approximation as indicated. Solid lines: κ and χ calculated from the definitions (42) and (44). Dashed lines: κ and χ calculated from the Fermi-liquid representations (43) and (45).

$$\chi = \left. \frac{\partial m}{\partial b} \right|_{b=0} \quad (44)$$

is given by the expression

$$\chi = \rho(0) \left(2 - \frac{\partial(\Sigma_{\uparrow}(0) - \Sigma_{\downarrow}(0))}{\partial b} \right). \quad (45)$$

These equations provide two more exact Fermi-liquid relations.

To calculate the spin susceptibility according to Eq. (44), the formalism has to be generalized for the spin-polarized case. Consider a constant external magnetic field b in z -direction which couples to the total spin

$$H = H_0 - 2bS_z = H_0 - b \sum_{i\sigma} q_{\sigma} n_{i\sigma}, \quad (46)$$

where $H_0 = H(b=0)$ is the Hamiltonian (1), $n_{i\sigma} = c_{i\sigma}^{\dagger} c_{i\sigma}$, and $q_{\uparrow} = 1$, $q_{\downarrow} = -1$ is a sign factor. The field strength is given by b . To account for a finite b in the formalism it is sufficient to redefine the on-site hopping $t_0 \mapsto t_{0\sigma} = t_0 - q_{\sigma} b$ and likewise $\epsilon_d \mapsto \epsilon_{d\sigma} = \epsilon_d - q_{\sigma} b$. Furthermore, the bath parameters may become spin dependent: $\epsilon_c \mapsto \epsilon_{c\sigma}$ and $V \mapsto V_{\sigma}$ in the impurity model (4). The self-consistency conditions (14) and (22) now read

$$n_{d\sigma} \equiv \langle d_{\sigma}^{\dagger} d_{\sigma} \rangle \stackrel{!}{=} n_{\sigma} \equiv \langle n_{i\sigma} \rangle, \quad V_{\sigma}^2 \stackrel{!}{=} z_{\sigma} M_2^{(0)}. \quad (47)$$

The magnetization is given by $m = n_{\uparrow} - n_{\downarrow}$.

Figure 7 shows the filling dependence of κ and χ as calculated from Eqs. (42) and (44) to be compared with κ and χ

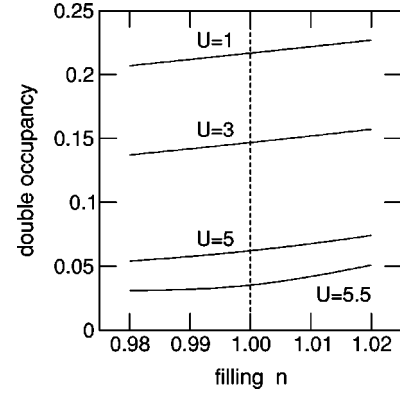


FIG. 8. Filling dependence of the double occupancy $d = \langle n_{\uparrow} n_{\downarrow} \rangle$ close to half-filling for different U .

as calculated from Eqs. (43) and (45). For $U=4$ there are hardly any differences. Small differences of the order of a few percent are found for $U=8$ (not shown). On the other hand, within the Hubbard-I approach the filling-dependence of κ and χ strongly depends on the way it is calculated. The respective results are shown in Fig. 7 for comparison.

Concluding, one can state that the Luttinger theorem as well as certain Fermi-liquid relations are well respected by the two-site DMFT. The same holds for the question of thermodynamic consistency: Although the two-site DMFT cannot be derived from an explicit thermodynamic potential, consistency relations such as

$$\frac{\partial^2 E}{\partial U \partial n} = \left. \frac{\partial \mu}{\partial U} \right|_n = \left. \frac{\partial \langle n_{\uparrow} n_{\downarrow} \rangle}{\partial n} \right|_U \quad (48)$$

are found to hold to a comparatively good approximation. An example is shown in Fig. 8. At half-filling the chemical potential is given by $\mu = U/2$. Therefore, as a function of the filling the double occupancy $\langle n_{\uparrow} n_{\downarrow} \rangle$ should have the slope $\partial \langle n_{\uparrow} n_{\downarrow} \rangle / \partial n = 1/2$ at $n=1$ for any (fixed) U . To a very good approximation this is reproduced by the results in Fig. 8.

IV. CONCLUSIONS

The two-site DMFT can be characterized as an approximate DMFT scheme which refers to a single-impurity Anderson model consisting of two sites only, one impurity and one bath site. Obviously, with a two-site SIAM the original self-consistency condition of the full DMFT can no longer be fulfilled, and consequently a comparatively crude approximation has to be tolerated. The idea, however, is to construct in this way the most simple approach that keeps the essence of the DMFT, namely the mapping onto an effective impurity model the bath parameters of which are determined self-consistently. In fact, for the single-band Hubbard model some of the calculations can be performed even analytically and there are no serious problems to be expected for a numerical treatment of multiband models.

Any realization of the DMFT requires a repeated solution of the impurity model which itself poses a complex many-body problem. An exact and unproblematic solution is possible for a SIAM with a finite, small number of degrees of

freedom—at the expense of an approximate mapping. This idea of the two-site DMFT is similar in spirit to the that of the exact-diagonalization method which aims at a minimization of the errors due to the discretization of the hybridization function by including as many sites n_s as feasible numerically. Contrary, the two-site DMFT stays with the case $n_s=2$ and can thus be considered as a “two-site ED” method. The latter, however, is not unique as it depends on the fit procedure used for the numerical determination of the bath parameters.^{14,15} The advantage of the two-site DMFT is that it is based on well motivated self-consistency conditions to fix the bath.

In principle, an extension of the two-site DMFT towards an n_s -site DMFT is conceivable for the single-band Hubbard model. This requires the consideration of higher-order terms in the high- and low-frequency expansion of the original self-consistency equation to fix the additional $2n_s-4$ bath parameters. The computational effort, however, grows exponentially with increasing n_s . Furthermore, higher-order static correlation functions would appear in the $1/\omega$ expansion of the on-site lattice Green function (13). At the order $1/\omega^4$ the correlated-hopping correlation function $B_\sigma \propto \sum_{i \neq j} t_{ij} \langle c_{i\sigma}^\dagger c_{j\sigma} (2n_i - \sigma - 1) \rangle$ can be expressed rigorously in terms of $G(\omega)$ by a sum rule³¹ similar to Eq. (15). At still higher orders, however, additional approximations must be tolerated.

The implementation of the two-site DMFT is straightforward, and the numerics is stable for the entire parameter space. It has to be stressed that the approach allows for computations that are faster by several orders of magnitude compared to numerically exact approaches such as the QMC or ED method. This advantage qualifies the approach for comprehensive investigations as are necessary, e.g., for the determination of phase diagrams. In this respect it is comparable with the iterative perturbation theory (IPT),^{4,18,19} for example.

The single-band Hubbard model has been considered here to illustrate the construction of the theory and to show up its advantages and limitations. Obviously, for the mere single-band model, the two-site DMFT cannot really compete against other more suitable methods. The main field of application are multiband Hubbard-type models which require the solution of more complicated effective impurity problems, or lattice models with reduced translational symmetry where one has to solve different impurity problems simultaneously.^{28,29} Opposed to the IPT,²² for example, the extension of the two-site DMFT to the multiband case is straightforward. Still the computational effort will be extremely small as compared to the numerically exact approaches.

Taking the mass-enhancement factor $m^*/m = z^{-1}$ as a measure for the strength of correlation effects, the Mott-transition point $n=1$ and $U=U_c$ obviously has a distinguished position in the phase diagram. Here the two-site DMFT reduces to the previously developed linearized DMFT (Ref. 25) which rather accurately predicts (the mean-field) U_c for the Hubbard model on different lattices^{25,28,29} and also for multiband models.^{26,27} The two-site DMFT can be considered as an extension of the linearized DMFT to the entire

parameter space. It interpolates between the Mott-transition point where $z=0$ and the uncorrelated limit $U=0$ or $n=0$ where $z=1$. Similar as the linearized theory, however, it cannot be controlled by a “small parameter” but is based on a physically motivated approximation.

The two-site DMFT is the most simple approach that describes the transition from the Mott insulating state to the Fermi liquid as a bifurcation scenario:⁴ At half-filling and for $U > U_c$ the approach reduces to the Hubbard-I approximation and yields the Mott-insulating solution. At $U = U_c$ a metallic solution splits off from the insulating one, the former being stable for $U < U_c$. Below U_c the two-site DMFT predicts a Fermi-liquid state with $z = 1 - U^2/U_c^2$. This is the same as the Brinkman-Rice-Gutzwiller result³³ (albeit with a different U_c). Although conceptually the two-site DMFT is quite different from the Gutzwiller method,^{8,37} the results for dependence of z on U and n are very similar. In particular, both approaches yield $z(\delta) - z(0) \propto \delta^2$ for $U < U_c$ and $z(\delta) - z(0) \propto \delta$ for $U > U_c$ in the limit $\delta = 1 - n \rightarrow 0$ (see Fig. 4 and Ref. 38).

Similar as the IPT but opposed to the Gutzwiller method, the two-site DMFT does not respect the Luttinger sum rule for the invariance of the Fermi-surface volume since it is not a conserving theory in the sense of Baym and Kadanoff³⁹ and cannot be derived from an explicit expression for a thermodynamic potential. On the other hand, it is remarkable that the deviations from the Luttinger sum rule and also the deviations from different exact Fermi-liquid and thermodynamical consistency relations are rather small. The comparison with the Hubbard-I approximation (which drastically violates these relations) suggests that this is due to the appearance of the quasiparticle peak in the spectral function. The Hubbard-I approximation can be considered as a local impurity approximation: The exact self-energy of the single-site (atomic) model is taken as an approximation for the self-energy of the lattice model. This approach and similar but improved theories^{42,43} yield high-frequency excitations such as the Hubbard bands but fail to reproduce Fermi-liquid properties at low frequencies. To get the (low-frequency) quasiparticle peak in addition and to restore the Fermi-liquid physics qualitatively, it is sufficient to couple merely a single (bath) degree of freedom to the single-site model. This also holds for the multiband case. A fully conserving and consistent theory, however, can only be obtained by coupling to an infinite number of bath sites as in the full DMFT.

Concluding, the two-site DMFT is a simple but non-perturbative mean-field approach to correlated lattice models. Compared to the full DMFT and to exact Fermi-liquid and thermodynamic relations, it yields satisfactory results for the Mott transition and the Fermi-liquid phase in the single-band Hubbard model with a minimum computational effort. The quality of the method, when applied to different physical problems, is not clear *a priori* and has to be examined. In particular, a comparison between the two-site and the full DMFT concerning magnetic order in the single-band model as well as the question of finite temperatures are intended for the future. Primarily, future applications shall address the manifestly complex phase diagrams for spin, charge and orbital order in multiband Hubbard-type models. Here the two-

site DMFT may serve to give a quick and comprehensive though rough overview of the main physics which can complement more thorough but selective studies.

ACKNOWLEDGMENT

This work is supported by the Deutsche Forschungsgemeinschaft within the Sonderforschungsbereich 290.

APPENDIX: MULTIBAND MODELS

The most general multiband model with on-site interaction reads

$$H = \sum_{i_1 i_2 \alpha_1 \alpha_2 \sigma} t_{i_1 i_2 \alpha_1 \alpha_2} c_{i_1 \alpha_1 \sigma}^\dagger c_{i_2 \alpha_2 \sigma} + \frac{1}{2} \sum_{i \sigma \sigma'} \sum_{\alpha_1 \alpha_2 \alpha_3 \alpha_4} U_{\alpha_1 \alpha_2 \alpha_3 \alpha_4} c_{i \alpha_1 \sigma}^\dagger c_{i \alpha_2 \sigma'}^\dagger c_{i \alpha_3 \sigma'} c_{i \alpha_4 \sigma}. \quad (\text{A1})$$

In most cases it is sufficient to take into account interaction parameters that are labeled by two indices, the direct interaction $U_{\alpha\alpha'} = U_{\alpha\alpha'\alpha\alpha'}$ and the exchange interactions $J_{\alpha\alpha'} = U_{\alpha\alpha'\alpha'\alpha}$ and $J'_{\alpha\alpha'} = U_{\alpha\alpha\alpha'\alpha'}$. Here $\alpha = 1, \dots, r$ is an orbital index, and r denotes the number of orbitals. Fourier transformation of the hopping $t_{ii'\alpha\alpha'}$ to \mathbf{k} space yields the free Hamilton matrix $t_{\alpha\alpha'}(\mathbf{k})$ the eigenvalues of which represent the free band structure $\epsilon_m(\mathbf{k})$, where $m = 1, \dots, r$ is the band index. The orbitally resolved free density of states is given by

$$\rho_{0,\alpha}(\omega) = \frac{1}{L} \sum_{\mathbf{k}m} |\phi_{\alpha m}(\mathbf{k})|^2 \delta[\omega - \epsilon_m(\mathbf{k})], \quad (\text{A2})$$

where $\phi_{\alpha m}(\mathbf{k})$ is the α th component of the m th eigenstate at each \mathbf{k} , namely, $\sum_{\alpha\alpha'} \phi_{\alpha m}(\mathbf{k})^* t_{\alpha\alpha'}(\mathbf{k}) \phi_{\alpha' m'}(\mathbf{k}) = \epsilon_m(\mathbf{k}) \delta_{mm'}$.

Assuming the self-energy to be local, it is easy to see from the usual diagram expansion that it must be diagonal with respect to the orbital index $\sum_{\alpha\alpha'} \Sigma_{\alpha\alpha'}(\omega) = \delta_{\alpha\alpha'} \Sigma_{\alpha\alpha}(\omega)$. Consider a cubic lattice and let α refer to orbitals with an angular dependence given by the cubic harmonics. The lattice symmetries then require the on-site ($i=i'$) elements of the lattice Green function $G_{ii'\alpha\alpha'\sigma}(\omega) = \langle\langle c_{i\alpha\sigma}; c_{i'\alpha'\sigma}^\dagger \rangle\rangle_\omega$ to be diagonal with respect to α :

$$G_{ii\alpha\alpha'\sigma}(\omega) = \delta_{\alpha\alpha'} G_{\alpha\sigma}(\omega). \quad (\text{A3})$$

Using the Dyson equation, the on-site Green function can generally be written as

$$G_{\alpha\sigma}(\omega) = \frac{1}{L} \sum_{\mathbf{k}} \left[\frac{1}{\omega + \mu - \mathbf{t}(\mathbf{k}) - \Sigma_{\alpha\sigma}(\omega)} \right]_{\alpha\alpha}. \quad (\text{A4})$$

Here $\Sigma_{\alpha\sigma}(\omega)$ is the (\mathbf{k} independent) diagonal $r \times r$ self-energy matrix and $\mathbf{t}(\mathbf{k})$ the \mathbf{k} -dependent (nondiagonal) free Hamilton matrix with the elements $t_{\alpha\alpha'}(\mathbf{k})$.

Within the DMFT the model (A1) can be mapped onto the following impurity model:

$$H_{\text{imp}} = \sum_{\alpha\sigma} \epsilon_{d\alpha} d_{\alpha\sigma}^\dagger d_{\alpha\sigma} + \frac{1}{2} \sum_{\sigma\sigma'} \sum_{\alpha_1 \alpha_2 \alpha_3 \alpha_4} U_{\alpha_1 \alpha_2 \alpha_3 \alpha_4} d_{\alpha_1 \sigma}^\dagger d_{\alpha_2 \sigma'}^\dagger d_{\alpha_3 \sigma'} d_{\alpha_4 \sigma} + \sum_{\alpha\sigma, k=2}^{n_s} \epsilon_{k\alpha\sigma} a_{k\alpha\sigma}^\dagger a_{k\alpha\sigma} + \sum_{\alpha\sigma, k=2}^{n_s} V_{k\alpha\sigma} (d_{\alpha\sigma}^\dagger a_{k\alpha\sigma} + \text{H.c.}), \quad (\text{A5})$$

with $\epsilon_{d\alpha} = t_{0\alpha} = t_{ii\alpha}$. The impurity Green function $G_{\text{imp},\alpha\sigma}(\omega) = \langle\langle d_{\alpha\sigma}; d_{\alpha\sigma}^\dagger \rangle\rangle_\omega$ is given by

$$G_{\text{imp},\alpha\sigma}(\omega) = \frac{1}{\omega + \mu - \epsilon_{d\alpha} - \Delta_{\alpha\sigma}(\omega) - \Sigma_{\text{imp},\alpha\sigma}(\omega)}. \quad (\text{A6})$$

The hybridization function $\Delta_{\alpha\sigma}(\omega) = \sum_k V_{k\alpha\sigma}^2 / (\omega + \mu - \epsilon_{k\alpha\sigma})$ and the impurity self-energy are diagonal with respect to α .

The lattice self-energy can be derived by functional differentiation from the Luttinger-Ward functional, $T \sum_{i'i\alpha'\alpha\sigma}(i\omega) = \delta\Phi / \delta G_{ii'\alpha\alpha'\sigma}(i\omega)$.⁴⁰ For any finite-dimensional lattice the DMFT consists in the assumption that the self-energy be local. This implies that Φ depends on the on-site propagator $G_{\alpha\sigma}(\omega)$ only. Hence, the functional Φ and thus the functional $\mathcal{S} = \delta\Phi / \delta G$ are the same for both, the lattice model ($\Sigma = \mathcal{S}[G]$) and the impurity model ($\Sigma_{\text{imp}} = \mathcal{S}[G_{\text{imp}}]$). One can proceed as for the single-band case: If the bath parameters $\epsilon_{k\alpha\sigma}$ and $V_{k\alpha\sigma}$ are chosen such that

$$\Delta_{\alpha\sigma}(\omega) = \omega + \mu - \epsilon_{d\alpha} - \Sigma_{\text{imp},\alpha\sigma}(\omega) - \frac{1}{G_{\alpha\sigma}(\omega)}, \quad (\text{A7})$$

i.e., such that the DMFT self-consistency condition

$$G_{\text{imp},\alpha\sigma}(\omega) = G_{\alpha\sigma}(\omega), \quad (\text{A8})$$

is fulfilled, then at once $\Sigma_{\text{imp},\alpha\sigma}(\omega) = \Sigma_{\alpha\sigma}(\omega)$, and the usual self-consistent procedure can be set up.

If different orbitals are equivalent due to lattice symmetries as, for example, the three t_{2g} orbitals in a cubic d -band system, one can make use of some simplifications: The self-energy $\Sigma_{\alpha\sigma}(\omega) = \Sigma_{\sigma}(\omega)$ and the DOS $\rho_{0,\alpha}(\omega) = \rho_0(\omega)$ are independent of the orbital index, and the on-site Green function is simply given by

$$G_{\alpha\sigma}(\omega) = G_{\sigma}(\omega) = \int_{-\infty}^{\infty} dx \frac{\rho_0(x)}{\omega + \mu - x - \Sigma_{\sigma}(x)}. \quad (\text{A9})$$

The lattice model can be mapped onto a simpler impurity model with $\epsilon_{k\alpha\sigma} = \epsilon_{k\sigma}$ and $V_{k\alpha\sigma} = V_{k\sigma}$. In this case the hybridization function and the impurity self-energy are α -independent, consistent with Eq. (A7).

The two-site DMFT is constructed straightforwardly. The number of (twofold spin-degenerate) one-particle orbitals in the impurity model is $M = r + r(n_s - 1) = rn_s$. For $n_s = 2$ and

for the general case of r nonequivalent orbitals there are (for each spin direction) $2r$ bath parameters to be determined, the one-particle energies $\epsilon_{\alpha\sigma}$ and the hybridization strengths $V_{\alpha\sigma}$ for $\alpha=1, \dots, r$. The comparison of the high-frequency expansions of $\Sigma_{\alpha\sigma}(\omega)$ and $\Sigma_{\text{imp},\alpha\sigma}(\omega)$ to lowest order leads to a first set of r self-consistency conditions

$$n_{d,\alpha\sigma} \equiv \langle d_{\alpha\sigma}^\dagger d_{\alpha\sigma} \rangle = n_{\alpha\sigma} \equiv \langle c_{i\alpha\sigma}^\dagger c_{i\alpha\sigma} \rangle \quad (\text{A10})$$

with $n_{\alpha\sigma} = (-1/\pi) \int_{-\infty}^0 \text{Im} G_{\alpha\sigma}(\omega + i0^+) d\omega$.

In the low-frequency limit the self-energy is expanded as $\Sigma_{\alpha\sigma}(\omega) = a_{\alpha\sigma} + (1 - z_{\alpha\sigma}^{-1})\omega + \mathcal{O}(\omega^2)$ where $z_{\alpha\sigma}$ is the orbital-dependent quasi-particle weight. Inserting the self-energy expansion up to the linear order into Eqs. (A4) and (A6), yields the respective coherent parts of the on-site lattice and the impurity Green function. Analogous to the single-band case one gets

$$G_{\text{imp},\alpha\sigma}^{(\text{coh})}(\omega) = \frac{z_{\alpha\sigma}}{\omega} + \frac{z_{\alpha\sigma}^2(\epsilon_{d\alpha} - \mu + a_{\alpha\sigma})}{\omega^2} + \frac{z_{\alpha\sigma}^2 V_{\alpha\sigma}^2 + z_{\alpha\sigma}^3(\epsilon_{d\alpha} - \mu + a_{\alpha\sigma})^2}{\omega^3} + \mathcal{O}(1/\omega^4). \quad (\text{A11})$$

The expansion of the coherent on-site lattice Green function, however, is slightly different:

$$G_{\alpha\sigma}^{(\text{coh})}(\omega) = \frac{z_{\alpha\sigma}}{\omega} + \frac{z_{\alpha\sigma}^2(t_{0\alpha} - \mu + a_{\alpha\sigma})}{\omega^2} + \frac{z_{\alpha\sigma}^3(t_{0\alpha} - \mu + a_{\alpha\sigma})^2}{\omega^3} + z_{\alpha\sigma}^2 \sum_{i'i'} t_{ii'\alpha\alpha'} z_{\alpha'\sigma} t_{i'i\alpha\alpha'} \frac{1}{\omega^3} + \mathcal{O}(1/\omega^4). \quad (\text{A12})$$

From the comparison one obtains the second set of r self-consistency conditions

$$V_{\alpha\sigma}^2 = \sum_{i'i'} z_{\alpha'\sigma} t_{ii'\alpha\alpha'}^2. \quad (\text{A13})$$

This includes an additional coupling of the different orbitals. Both self-consistency conditions (A10) and (A13) reduce to Eq. (47) for the single-band case.

*Email address: michael.potthoff@physik.hu-berlin.de

¹ A. Georges and G. Kotliar, Phys. Rev. B **45**, 6479 (1992).

² M. Jarrell, Phys. Rev. Lett. **69**, 168 (1992).

³ T. Pruschke, M. Jarrell, and J.K. Freericks, Adv. Phys. **44**, 187 (1995).

⁴ A. Georges, G. Kotliar, W. Krauth, and M.J. Rozenberg, Rev. Mod. Phys. **68**, 13 (1996).

⁵ W. Metzner and D. Vollhardt, Phys. Rev. Lett. **62**, 324 (1989).

⁶ D. Vollhardt, Int. J. Mod. Phys. B **3**, 2189 (1989).

⁷ J. Hubbard, Proc. R. Soc. London, Ser. A **276**, 238 (1963).

⁸ M.C. Gutzwiller, Phys. Rev. Lett. **10**, 159 (1963).

⁹ J. Kanamori, Prog. Theor. Phys. **30**, 275 (1963).

¹⁰ M. Ulmke, Eur. Phys. J. B **1**, 301 (1998).

¹¹ D. Vollhardt, N. Blümer, K. Held, M. Kollar, J. Schlipf, and M. Ulmke, Z. Phys. B **103**, 283 (1997).

¹² T. Obermeier, T. Pruschke, and J. Keller, Phys. Rev. B **56**, 8479 (1997).

¹³ M.J. Rozenberg, X.Y. Zhang, and G. Kotliar, Phys. Rev. Lett. **69**, 1236 (1992).

¹⁴ M. Caffarel and W. Krauth, Phys. Rev. Lett. **72**, 1545 (1994).

¹⁵ Q. Si, M.J. Rozenberg, G. Kotliar, and A.E. Ruckenstein, Phys. Rev. Lett. **72**, 2761 (1994).

¹⁶ R. Bulla, A.C. Hewson, and T. Pruschke, J. Phys.: Condens. Matter **10**, 8365 (1998).

¹⁷ R. Bulla, Phys. Rev. Lett. **83**, 136 (1999).

¹⁸ H. Kajueter and G. Kotliar, Phys. Rev. Lett. **77**, 131 (1996).

¹⁹ M. Potthoff, T. Wegner, and W. Nolting, Phys. Rev. B **55**, 16 132 (1997).

²⁰ T. Pruschke, D.L. Cox, and M. Jarrell, Phys. Rev. B **47**, 3553 (1993).

²¹ G. Hülsenbeck and F. Stephan, Z. Phys. B: Condens. Matter **94**,

281 (1994).

²² A.I. Lichtenstein and M.I. Katsnelson, Phys. Rev. B **57**, 6884 (1998).

²³ T. Maier, M.B. Zöfl, T. Pruschke, and J. Keller, Eur. Phys. J. B **7**, 377 (1999).

²⁴ E. Lange, Mod. Phys. Lett. B **12**, 915 (1998).

²⁵ R. Bulla and M. Potthoff, Eur. Phys. J. B **13**, 257 (2000).

²⁶ K. Held and R. Bulla, Eur. Phys. J. B **17**, 7 (2000).

²⁷ Y. Ono, R. Bulla, and A.C. Hewson, Eur. Phys. J. B **19**, 375 (2001).

²⁸ M. Potthoff and W. Nolting, Eur. Phys. J. B **8**, 555 (1999).

²⁹ M. Potthoff and W. Nolting, Phys. Rev. B **60**, 7834 (1999).

³⁰ E. Müller-Hartmann, Z. Phys. B: Condens. Matter **76**, 211 (1989).

³¹ M. Potthoff, T. Herrmann, T. Wegner, and W. Nolting, Phys. Status Solidi B **210**, 199 (1998).

³² G. Moeller, Q. Si, G. Kotliar, M. Rozenberg, and D.S. Fisher, Phys. Rev. Lett. **74**, 2082 (1995).

³³ W.F. Brinkman and T.M. Rice, Phys. Rev. B **2**, 4302 (1970).

³⁴ M. Potthoff, Habilitation thesis, Humboldt University, Berlin, 2000.

³⁵ A. Georges and W. Krauth, Phys. Rev. B **48**, 7167 (1993).

³⁶ M. Jarrell and T. Pruschke, Z. Phys. B: Condens. Matter **90**, 187 (1993).

³⁷ M.C. Gutzwiller, Phys. Rev. **137**, A1726 (1965).

³⁸ D. Vollhardt, P. Wölfle, and P.W. Anderson, Phys. Rev. B **35**, 6703 (1987).

³⁹ G. Baym and L.P. Kadanoff, Phys. Rev. **124**, 287 (1961).

⁴⁰ J.M. Lutinger and J.C. Ward, Phys. Rev. **118**, 1417 (1960).

⁴¹ J. Beenen and D.M. Edwards, Phys. Rev. B **52**, 13 636 (1995).

⁴² L.M. Roth, Phys. Rev. **184**, 451 (1969).

⁴³ W. Nolting and W. Borgiel, Phys. Rev. B **39**, 6962 (1989).